Available online at www.sciencedirect.com
ScienceDirect
Bioorganic & Medicinal Chemistry Letters 17 (2007) 486–490
Bioorganic & Medicinal Chemistry Letters

Structure–activity relationships of novel non-competitive mGluR1 antagonists: A potential treatment for chronic pain

Dafydd R. Owen,* Peter G. Dodd, Simon Gayton, Ben S. Greener, Gareth W. Harbottle, Simon J. Mantell, Graham N. Maw, Simon A. Osborne,† Huw Rees, Tracy J. Ringer, Margarita Rodriguez-Lens and Graham F. Smith

Pfizer Global Research and Development, Ramsgate Road, Sandwich, CT13 9NJ, UK

Received 22 August 2006; revised 9 October 2006; accepted 9 October 2006
Available online 11 October 2006

Abstract—A series of novel mGluR1 antagonists have been prepared. Incorporation of fragments derived from weak lead matter into a library led to enhanced potency in a new chemical series. A chemistry driven second library iteration, covering a greatly enhanced area of chemical space, maintained good potency and introduced metabolic stability.

Glutamate acts at two distinct classes of receptor; fast neurotransmission is mediated by ion channel coupled 'ionotropic' receptors that are widely distributed throughout the central nervous system (CNS). Glutamate can also activate G-protein coupled 'metabotropic' receptors (mGluRs). There are eight mGluR receptor subtypes that have been divided into three groups by sequence homology and intracellular coupling. The mGluRs demonstrate distinct patterns of distribution raising the possibility that ligands acting at distinct subtypes could have selective effects. The group I mGluRs consisting of mGluR1 and mGluR5 are coupled to phospholipase C, causing release of intracellular Ca^{2+} and activation of protein kinase C. Recent data have implicated group I mGluR receptors in sensory processing. In particular receptor antagonists of the mGluR1 subtype have been reported to be analgesic.[1–3] Further evidence suggests that activation of the mGluR1 receptor mediates hyperalgesia seen in neuropathic and capsaicin-induced pain states.[2–5] The mGluR1 receptor is located post-synaptically on glutamatergic synapses and functions to increase excitability under conditions of high frequency stimulation and/or excessive glutamate thus making the neurone more sensitive to NMDA-R mediated excitotoxicity. Therefore, antagonising mGluR1 is also predicted to be neuroprotective.

The first class of mGluR1 antagonists identified were amino acid based derivatives that displace glutamate directly from the receptor.[6] Given the expected requirement of having to achieve CNS penetration to attain pain efficacy through this mechanism, this structural class makes the challenge difficult, but not impossible.[7] Many non-amino acid based mGluR1 antagonists have also been identified over the last few years. These represent a better starting point for a CNS penetrant approach. An example of such a non-amino acid based structure is CPCCOEt which was found to be a non-competitive antagonist.[8] This compound was found to modulate mGluR1 activity through binding at an allosteric site. Further examples of non-amino acid based mGluR1 active templates are shown in Figure 1 and include quinazoline derivatives,[9] azepines,[10] triazafluorenones,[11] and quinoxalines.[12]

Directed screening of selected file compounds in our mGluR1[13] assay led to the discovery of several weakly active compounds (Table 1).

The amine-derived substituents (R, Table 1) of the weak, amidic leads (A, Table 1) were chosen for further development using library synthesis methods. The four amines **1**–**4** (Table 1) were combined with 125 heterocyclic

Keywords: mGluR; mGluR1; CNS; Chronic pain; Library; Quinoxaline; Pyrazine; clog *P*; log *D*; Metabolism.
* Corresponding author. Tel.: +44 1304648445; e-mail: dafydd.owen@pfizer.com
† Present address: MRC Technology, 1-3 Burtonhole Lane, Mill Hill, London, NW7 1AD, UK.

0960-894X/$ - see front matter © 2006 Elsevier Ltd. All rights reserved.
doi:10.1016/j.bmcl.2006.10.015

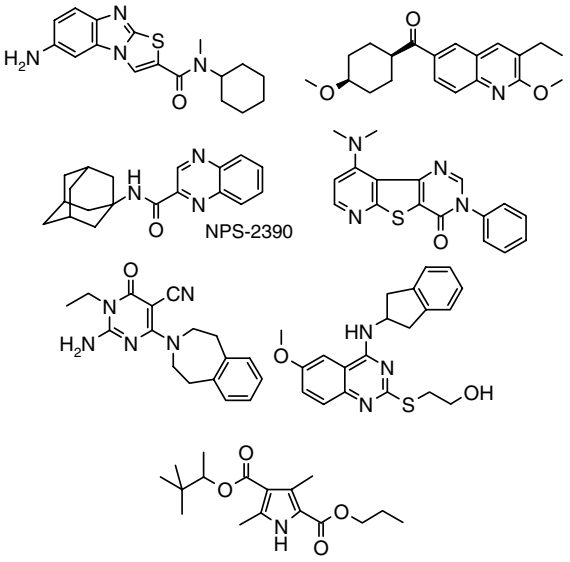

Figure 1.

Table 1.

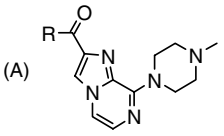

Compound	R/amine	K_i (nM)
1	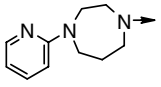	407
2	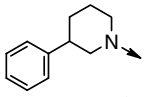	1085
3	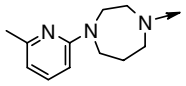	650
4	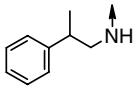	1204

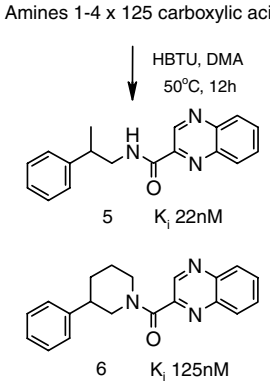

Scheme 1.

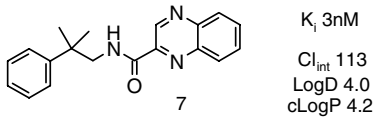

Figure 2.

carboxylic acid derivatives, each of molecular weight <250, in a simple amide bond forming protocol. This resulted in the identification of two key leads, **5** and **6**, of increased potency (Scheme 1).

The quinoxaline-2-carboxylic acid had previously been identified as an active mGluR1 fragment by others in compounds such as NPS-2390[12] (Fig. 1). The two stereoisomers of our own racemic quinoxaline amide **5** were found to be equipotent. The achiral, gem dimethyl analogue **7** was significantly more potent, but was shown to have poor human liver microsomal metabolic stability (Cl_{int} μl/min/mg, Fig. 2).[14] Given this lead, the key challenge for the programme was to retain potency, low molecular weight and introduce metabolic stability. This was to be achieved through a reduction in compound lipophilicity.

Further analogues were produced via amide bond formation looking at both the acid and amine portions. Analogues of the dimethylphenethylamine showed that the benzylic gem dimethyl group was optimal (**8**–**10**, Table 2) and that introducing benzylic heteroatoms cost potency (**11**), dramatically so in the case of amine **12**. Fluorination of the aromatic ring retained potency but failed to positively impact on the rapid metabolism seen in the series (**9**). A carbon to nitrogen switch in phenyl group also caused a loss in potency (**13**).

Table 2.

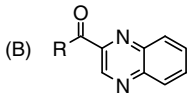

Compound	R	K_i (nM)
8	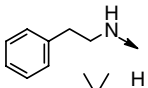	69
9	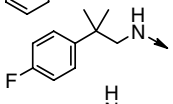	2
10	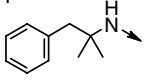	40
11	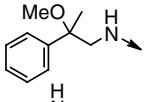	15
12	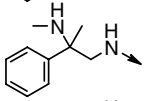	510
13	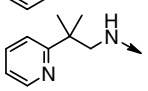	40

Table 3.

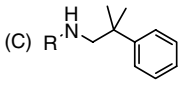

Compound	R	K_i (nM)
14		6550
15	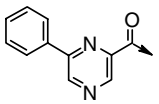	315
16	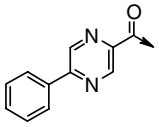	179
17	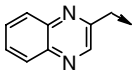	1210
18	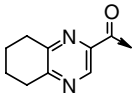	2

Table 4.

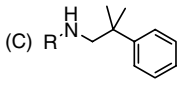

Compound	R	K_i (nM)	clog P	log D	Cl_{int}
15	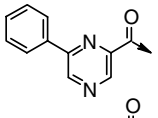	315	4.7	2.6	47
16	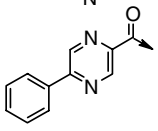	179	4.7	3.4	59
19	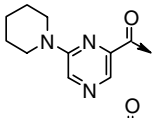	11	4.1	4.4	>440
20	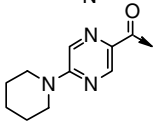	17	4.1	4.5	125

Within the acid portion, attempts to reduce lipophilicity also failed. Removing a fused ring, in going from quinoxaline to pyrazine **14** (Table 3), cost greater than 1000-fold in potency. However, branching the aryl in the 5- or 6-positions in pyrazines **15** and **16** did win some activity back. Loss of activity on removal of the amide carbonyl group ruled out another potential position for a basic centre (**17**).

Having established that high lipophilicity in the amide substituent was essential for good activity, increased hydrophilicity had to be found elsewhere in the compounds to make this a viable series. It was clear that operating at a clog $P > 4.0$ was regularly fulfilling our pharmacological requirements but was most unlikely to give metabolic stability of any utility.

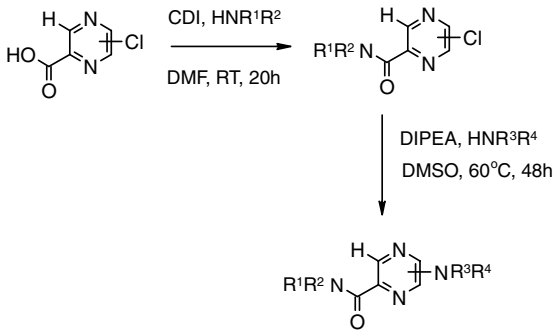

Scheme 2.

Despite the moderate potency of **15** and **16**, they were considered the most promising leads at the time. These regioisomers were reminiscent of an array of compounds previously synthesised using high-throughput chemistry as part of the company's file enrichment programme. It was proposed that the the C-5/C-6 phenyl groups in the pyrazine amides **15** and **16** could be replaced by an amine-derived substituent of similar lipophilicity. This changed the synthetic route to an amide coupling at the 2-carboxyl followed by an amine displacement of the 5- or 6-chloropyrazine. This had been the basis of the previously synthesised file enrichment array (Scheme 2).

Targeted screening of the 6000 compound array already on file gave more moderate potency hits. Encouragingly, on combining the phenethylamine amide substituent identified in our earlier library work, the potency of the singleton piperidine prototypes **19** and **20** both proved to be below 20 nM. This represented a greater than 10-fold improvement in potency from the biaryl leads **15** and **16** without having increased molecular weight at all (Table 4).

Using the established parallel synthesis protocol that had produced the initial array (Scheme 2), two targeted libraries, using the 5-chloro and 6-chloropyrazine cores, were produced. These were designed to look at the substituents at the two points of diversity presented by the simple pyrazine cores in a combinatorial fashion. The acids of both pyrazine cores were first reacted with five amines as in Scheme 2 to form amides. The regioisomeric chloroheterocyclic positions were then displaced by a large range of amines. The amine selection for the second step was designed to keep product clog P <4.8 and molecular weight <450. Over 500 compounds were synthesised in each library.

Both the C-5 and C-6 amino substituted pyrazine regioisomers gave potent compounds in their respective libraries. The dimethylphenethylamine from Figure 2 still proved to be the most reliable amide substituent in both templates. Of the most active C-6 amino analogues, all had poor metabolic stability (**21**–**26**, Table 5).

Table 5.

Compound		K_i (nM)	clog *P*	log *D*	Cl_{int}
21	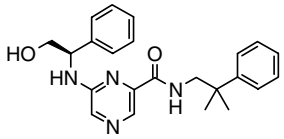	27	3.9	3.6	270
22	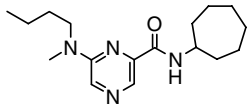	30	4.8	3.8	>440
23	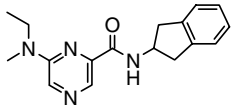	40	3.1	3.6	298
24	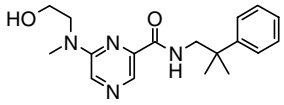	43	2.8	2.7	>440
25	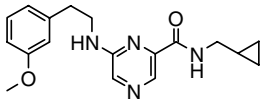	44	3.5	3.2	>440
26	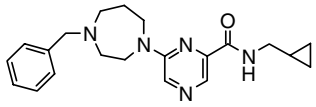	56	3.1	3.0	>440

Table 6.

Compound		K_i (nM)	clog *P*	log *D*	Cl_{int}
27	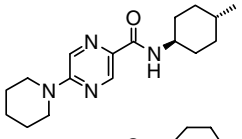	3	3.8	4.4	50
28	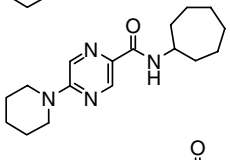	8	3.8	3.9	62
29	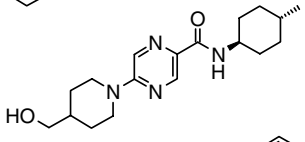	9	2.3	3.3	<7
30	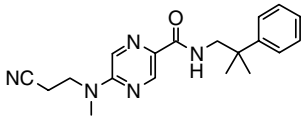	14	3.0	2.9	20
31	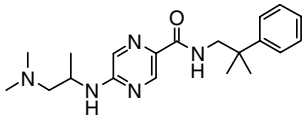	27	3.9	2.0	12
32	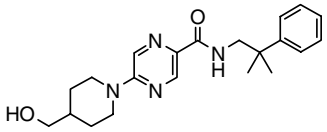	35	2.7	3.5	44

The *in vitro* metabolic profile of the C-5 amino substituted pyrazines was far more encouraging with compound **29** proving to be the most stable (Table 6). Within this sub-series there appeared to be a trend for the compounds of lower log *D* having better *in vitro* metabolic stability. There is a clear contrast in the metabolic profiles of the two regioisomeric C-5/C-6 amino sub-series (Tables 5 and 6).

Compound **29** has an attractive all round *in vitro* profile and showed good permeability as judged by the PAMPA assay (Passive transcellular diffusion rate: 25.5×10^{-6} cm/s). It is an attractive lead as it represents a potent, metabolically stable mGluR1 antagonist of low molecular weight.

In conclusion, fragments identified from in-house hits were carried into a range of simpler pyrazine-based cores through an amide library synthesis. Correlation of these leads to a second, previously synthesised array protocol allowed a designed library to identify versatile, synthetically simple, potent mGluR1 antagonists. Overall, highly lipophilic lead matter has been optimised, maintaining sub-10 nM potency while simultaneously reducing log *D*, attaining CNS drug-compatible molecular weight[15] and introducing metabolic stability to the series. Compound **29** may represent a useful lead in the ongoing search for mGluR1 antagonists for nociceptive pain.

References and notes

1. Salt, T. E.; Binns, K. E. *Neuroscience* **2000**, *100*, 375.
2. Neugebauer, V.; Chen, P. S.; Willis, W. D. *J. Neurophysiol.* **1999**, *82*, 272.
3. Fundytus, M. E.; Fisher, K.; Dray, A.; Henry, J. L.; Coderre, T. J. *Neuroreport* **1998**, *9*, 731.
4. Young, M. R.; Blackburn-Munro, G.; Dickinson, T.; Johnson, M. J.; Anderson, H.; Nakalembe, I.; Fleetwood-Walker, S. M. *J. Neurosci.* **1998**, *18*, 10180.
5. Fundytus, M. E.; Yashpal, K.; Chabot, J. G.; Osborne, M. G.; Lefebvre, C. D.; Dray, A.; Henry, J. L.; Coderre, T. J. *Br. J. Pharmacol.* **2001**, *132*, 354.
6. Pellicciari, R.; Luneia, R.; Costantino, G.; Marinozzi, M.; Natalini, B.; Jakobsen, P.; Kanstrup, A.; Lombardi, G.; Moroni, F.; Thomsen, C. *J. Med. Chem.* **1995**, *38*, 3717.
7. Schwarz, J. B.; Gibbons, S. E.; Graham, S. R.; Colbry, N. L.; Guzzo, P. R.; Le, V.; Vartanian, M. G.; Kinsora, J. J.; Lotarski, S. M.; Li, Z.; Dickerson, M. R.; Su, T.; Weber, M. L.; El-Kattan, A.; Thorpe, A. J.; Donevan, S. D.; Taylor, C. P.; Wustrow, D. J. *J. Med. Chem.* **2005**, *48*, 3026.
8. Litschig, S.; Gasparini, F.; Rueegg, D.; Stoehr, N.; Flor, P. J.; Vranesic, I.; Prézeau, L.; Pin, J.; Thomsen, C.; Kuhn, R. *Mol. Pharmacol.* **1999**, *55*, 453.
9. Ambler, S. J.; Baker, S. R.; Clark, B. P.; Coleman, D. S.; Foglesong, R. J.; Goldsworthy, J.; Jagdmann, G. E.; Johnson, K. W.; Kingston, A. E.; Owton, W. M.; Schoepp, D. D.; Hong, J. E.; Schkeryantz, J. M.; Vannieuwenhze, M. S.; Zia-Ebrahimi, M. S. WO2001032632.
10. Binggeli, A.; Maerki, H.; Mutel, V.; Wilhelm, M.; Wostl, W. WO2002051418.
11. Gomtsyan, A.; Bayburt, E. K.; Schmidt, R. G.; Zheng, G. Z.; Perner, R. J.; Didomenico, S.; Koenig, J. R.; Turner, S.; Jinkerson, T.; Drizin, I.; Hannick, S. M.; Macri, B. S.; McDonald, H. A.; Honore, P.; Wismer, C. T.; Marsh, K. C.; Wetter, J.; Stewart, K. D.; Oie, T.; Jarvis, M. F.; Surowy, C. S.; Faltynek, C. R.; Lee, C. *J. Med. Chem.* **2005**, *48*, 744.
12. Van Wagenen, B. C.; Moe, S. T.; Smith, D. L.; Sheehan, S. M.; Shcherbakova, I.; Travato, R.; Walton, R.; Barmore, R.; Delmar, E. G. WO2000073283.
13. The ability of the compounds to antagonise glutamate-evoked increases in calcium internalisation in a mGLuR1 expressing cell line may be measured using the following assay. Chinese Hamster Ovary cells, stably transfected with the rat mGluR1a receptor (CHO-1a), were used in the assay. CHO-1a cells were seeded onto shallow 96-well plates and assayed for confluency of 80–90%. Cells were loaded with Fluo-3-AM dye (8.8 mM final concentration; excitation 488 nM, emission 530 nM) in the presence of probenecid (2.5 mM) for 45–90 min at 37 °C, after which time excess dye was removed by washing. The cell plate was then loaded onto a fluorometric imaging plate reader (FLIPr, Molecular Devices). Baseline readings were measured for 30 s. Test compounds were added by the FLIPr and allowed to equilibrate for 5 min before the addition of a 40 mM glutamate challenge (this was the approximate ED_{90} for glutamate against the receptor expressed in these cells). Readings were taken for a further 2 min. Measurements were made of the area of peak obtained in response to the glutamate addition and inhibition curves were constructed. Glutamate dose–response curves were included on each experiment day to allow IC_{50} values to be converted to modified K_i values.
14. Korfmacher, W. A.; Palmer, C. A.; Nardo, C.; Dunn-Meynell, K.; Grotz, D.; Cox, K.; Lin, C.-C.; Elicone, C.; Liu, C.; Duchoslav, E. *Rapid Commun. Mass. Spectrom.* **1999**, *13*, 901.
15. Pajouhesh, H.; Lenz, G. R. *NeuroRx* **2005**, *2*, 541.